Japanese Journal of Applied Physics **57**, 126503 (2018)
https://doi.org/10.7567/JJAP.57.126503

REGULAR PAPER

Development of oxide thin-film transistor using all spin-on-glass insulators with addition of hydrogen peroxide: Buffer, gate insulator, and interlayer dielectric

Sang Ho Hwang[1*], Yeong Jo Baek[1], Min Taek Hong[1], Sang Min Lee[1], Ye Lin Han[2], Dong Sung Moon[3], Eui-Jung Yun[4], and Byung Seong Bae[1*]

[1]*School of Electronics and Display Engineering, Hoseo University, Asan, Chungnam 31499, Republic of Korea*
[2]*Department of NanoBiotronics, Hoseo University, Asan, Chungnam 31499, Republic of Korea*
[3]*DeepMagic Co., Ltd., Pixian, Chengdu, Sichuan 610097, China*
[4]*Department of ICT Automotive Engineering, Hoseo University, Dangjin, Chungnam 31702, Republic of Korea*

*E-mail: bsbae3@hoseo.edu

Received July 2, 2018; revised September 3, 2018; accepted September 12, 2018; published online November 9, 2018

A top-gate oxide thin-film transistor (TFT) with all spin-on-glass (SOG) insulators was developed. The SOG is based on methyl siloxane and was used for the buffer layer, gate insulator, and interlayer dielectric instead of a vacuum process. The SOG was diluted with ethanol, and a small amount of hydrogen peroxide was added. The diluted SOG was applied to top-gate amorphous indium–gallium–zinc-oxide TFTs, and the effects of the dilution and the hydrogen peroxide added were investigated. The TFTs with the optimized SOG insulators showed a mobility of 7.1 $cm^2/(V{\cdot}s)$, a threshold voltage of 0.5 V, a subthreshold slope of 0.1 V/dec, and an on/off current ratio of 3.6×10^7.

1. Introduction

Thin-film transistors (TFTs) are important components for display backplanes and sensing devices. In displays, TFTs are used for integrated drive circuits and switching elements. Recently, oxide TFTs have been receiving much attention owing to their higher mobility than amorphous silicon TFTs, lower cost than low temperature polysilicon (LTPS) TFTs, and solution processing.[1–3] For application in display backplanes, it is important to have low leakage current, low threshold voltage, high mobility, and good stability, which are mainly influenced by the quality of the gate insulator.[4–9] In conventional oxide TFTs, gate insulators such as SiO_2 and Al_2O_3 are formed by physical or chemical deposition, which are vacuum plasma processes.

Oxide semiconductors are sensitive to annealing conditions and the external environment. In the fabrication process, plasma ion-induced damage deteriorates electrical characteristics. Therefore, much attention is necessary during the deposition of an insulator on an oxide semiconductor to avoid ion-induced damage in top-gate structure TFTs.[10–12] In a vacuum process, energetic ions in the plasma bombard the active oxide material and generate defects.[13] One way to avoid this is to use a solution process instead of a vacuum process for the gate insulator.

A solution process does not generate plasma ions and is receiving more interest for next-generation displays because it is simple and inexpensive.[14–16] Gate insulators prepared by solution processes were applied to organic TFTs and polysilicon TFTs using materials such as olefin, perylene, and SU-8.[17–19] Other solution processes using spin-on-glass (SOG) have been reported.[20–23] A solution process with SOG based on methyl siloxane was investigated for oxide TFTs in which SOG was applied to all insulating layers such as buffer, gate insulator, and interlayer dielectric.

A SOG solution forms a silicate polymer array with a Si–O structure upon heat treatment in the range of 400–900 °C and has been widely used for the interlayer dielectric in semiconductor processes. SOG can be applied to a large substrate area and has an advantage of planarization. Passivation applications of SOG in oxide TFTs have been reported, but application to gate insulators is rare.

We developed amorphous indium–gallium–zinc-oxide (a-IGZO) TFTs with all insulators by the SOG process, that is, SOG for the buffer layer, gate insulator, and interlayer dielectric.[24–26] SOG was diluted to improve the performance of the TFT, and the effect of the dilution was investigated.[27] In addition, the effect of an oxidizing agent added to the SOG was investigated. It was reported that addition of nitric acid to an oxide precursor increased the mobility of the solution-based oxide TFT owing to the oxygen generated after the decomposition of nitric acid.[28] The metal cation bonds easily to oxygen anions supplied by the acid. In this study, a small amount of hydrogen peroxide was added, and the effect of hydrogen peroxide was investigated as an oxidizing agent similarly nitric acid.

2. Experimental methods

Figure 1 shows the developed top-gate IGZO TFT with SOG insulators. The SOG process was used for all the insulators, namely, the buffer layer, gate insulator, and interlayer dielectric. After cleaning the glass substrate, the buffer layer was formed by SOG. A 50-nm-thick IGZO active channel layer was deposited on the buffer layer by RF magnetron sputtering at room temperature using a sputter target at an In : Ga : Zn atomic ratio of 1 : 1 : 1. The layer was deposited under the following conditions: RF power of 50 W, working pressure of 5 mTorr, and O_2-to-Ar ratio of 25%.

The IGZO layer was patterned for the active channel by wet etching with buffered oxide etch (BOE) solution diluted

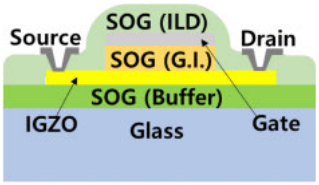

Fig. 1. (Color online) Cross-sectional structure of the top-gate TFT with SOG insulators.

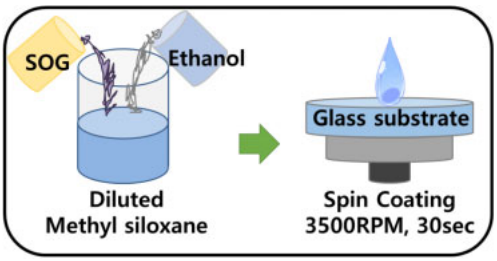

(a)

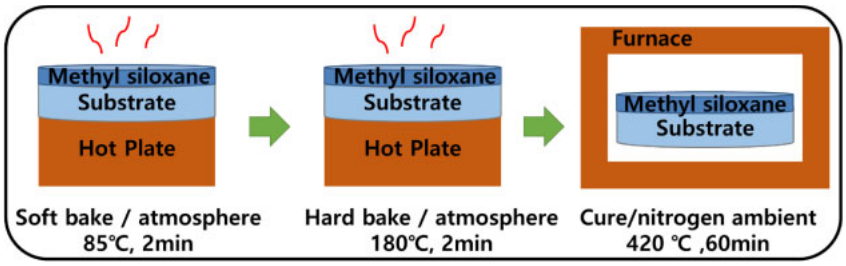

(b)

Fig. 2. (Color online) (a) Dilution of SOG and (b) SOG film formation process.

with deionized water at a ratio of 500 : 1. After patterning the IGZO active layer by photolithography, it was annealed at 250 °C for 1 h under O_2 atmosphere to reduce the oxygen vacancies and process-related defects.

After IGZO patterning, the SOG was spin-coated and cured for the gate insulator. On the gate insulator, a 100-nm-thick Cr layer was deposited by DC magnetron sputtering and patterned for the gate electrode by wet etching. Next, dry etching was used to etch away the gate insulator except for the part under the gate electrode. It was etched by reactive-ion etching (RIE) with the gate electrode as an etching mask. The RF power, etching time, and working pressure were 180 W, 270 s, and 100 mTorr, respectively. The etching gases were CF_4 and O_2 used at a ratio of 60 : 20.

After etching the gate insulator, the exposed IGZO layer was doped by oxygen plasma treatment in the IGZO source/drain region at room temperature for 30 s in an RIE chamber under the following process conditions: RF power of 180 W, O_2 flow rate of 60 sccm, and working pressure of 100 mTorr. The bombardment of reactive oxygen ions to the IGZO film results in many defects formed which increases carrier density. We measured the sheet resistance of the IGZO layer. It was unmeasurable before doping owing to its high resistivity. However, it decreased to 8.0 kΩ/sq after 30 s of doping.

After doping, the inter-layer dielectric was formed by the SOG process. Contact holes were then dry-etched to connect the source/drain regions of the IGZO layer to the source/drain metal electrodes. Before contact hole patterning, oxygen plasma treatment was carried out under the same conditions as doping to make the SOG surface hydrophilic. The dry etching conditions for the contact holes were the same as those used for the gate insulator. Next, a 150-nm-thick Al layer was deposited by DC magnetron sputtering and patterned for the source/drain electrodes by wet etching. The channel length and width were 20 and 40 μm, respectively. The TFT characteristics were measured in a dark box to avoid changes in the TFT characteristics induced by light illumination.

All the three insulating layers were formed by SOG. For the high performance of the TFT, the dilution was necessary. Figure 2(a) shows the SOG dilution and coating process. The SOG was diluted with ethanol at 80 °C at three dilution ratios: 0% (40 ml SOG), 50% (20 ml SOG + 20 ml ethanol), and 75% (10 ml SOG + 30 ml ethanol). The dilution was defined as ethanol/(SOG + ethanol). Next, 1 ml of hydrogen peroxide was added to each of the solutions to investigate its effects. The SOG solutions were spin-coated on the glass at 3500 rpm and then soft-baked at 80 °C for 1 min, followed by hard bake at 180 °C for 3 min as shown in Fig. 2(b).

After baking, final curing was carried out with the temperatures increased from 150 to 450 °C at intervals of 100 °C with curing for 15 min at each temperature. The curing conditions and dilution ratio were the same for the buffer, gate insulator, and inter-layer dielectric except for the curing temperature of 300 °C for the inter-layer dielectric. Curing promotes polymer cross linking, which provides mechanical integrity and film stability in subsequent processes.[29)]

For the undiluted SOG solution, the thickness of the layer was 340 nm. The diluted solutions were coated several times to obtain similar thicknesses. The 50% diluted SOG solution was coated two times, and the thickness measured was 238 nm. The 75% diluted SOG solution was coated 5 times, and the thickness measured was 238 nm. In the case of H_2O_2 addition, the thicknesses obtained for the 0, 50, and 75% diluted SOG solutions were 496, 335, and 335 nm, respectively.

3. Results and discussion

The top-gate oxide TFT shown in Fig. 1 was developed using the SOG process for all insulators, namely, the buffer, gate insulator, and interlayer dielectric. Among all three insulators, the gate insulator is the most important for the performance of the TFT because it contacts the IGZO layer to form the interface that becomes the channel of the TFT. The

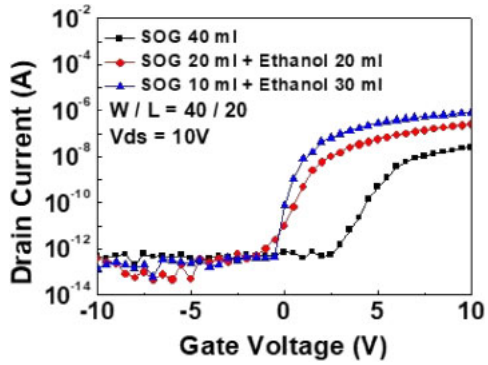

(a)

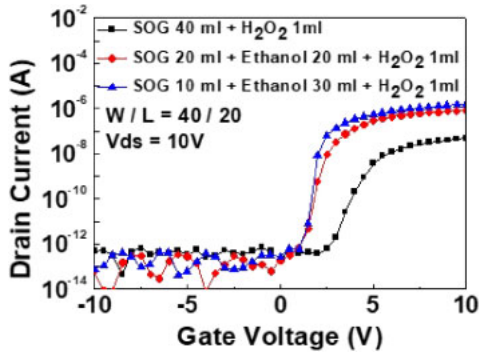

(b)

Fig. 3. (Color online) Transfer characteristic of oxide TFTs as a function of dilution ratio: (a) without addition of H_2O_2, (b) with addition of H_2O_2.

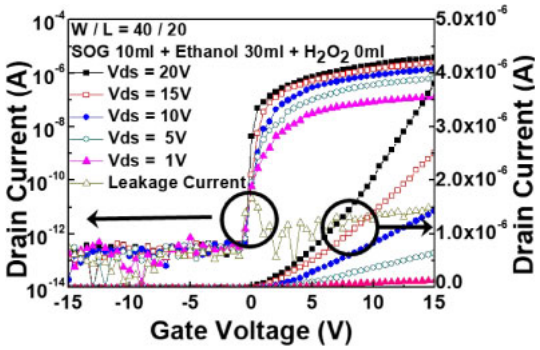

(a)

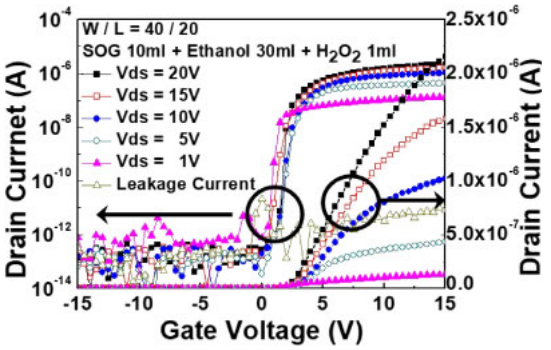

(b)

Fig. 4. (Color online) Transfer characteristics of oxide TFTs for various drain voltages with 75% dilution: (a) without addition of H_2O_2, (b) with addition of H_2O_2.

coating and curing conditions of the SOG significantly affect the characteristics of the TFT.

We compared the TFT characteristics obtained by varying the dilution ratio of the SOG: 0, 50, and 75%. Figure 3(a) shows the transfer characteristics at different dilution ratios of SOG, and Fig. 3(b) shows the transfer characteristics at different dilution ratios with the addition of hydrogen peroxide. The graph shows the improvement after dilution. Since the gate insulator thicknesses for each dilution were different, we examined the effect of the gate insulator thickness. The TFT current is proportional to the capacitance of the gate insulator, which means that the current is inversely proportional to the thickness of the gate insulator. The ratio of the thickness is 238 nm/340 nm. Therefore, the effect of the thickness is a 1.4-fold larger current for the diluted case. The curves show that the on-current is lowest for the TFT with the insulators from the undiluted SOG solution. The on-current of the diluted case is about two magnitude orders larger than undiluted case, which is much large compared to 1.4 owing to the thickness effect. That is, the dilution is necessary for the improvement of on-currents. The effect of H_2O_2 addition is shown in Fig. 3(b). As the dilution ratio increased, the on-currents increased also in the case of H_2O_2 addition, as shown in Fig. 3(b). Hydrogen peroxide is a strong oxidizing agent. Therefore, we consider that its addition results in the reduction in the number of oxygen vacancies and improve the TFT characteristics. With the addition of hydrogen peroxide, the on-current increased slightly and the subthreshold slope became steep, as shown in Fig. 3(b).

Figures 4(a) and 4(b) show the transfer characteristics of IGZO TFTs prepared using SOG diluted with ethanol (10 ml of SOG and 30 ml of ethanol). Figure 4(a) shows the results obtained without H_2O_2 addition, and Fig. 4(b) shows the results obtained with H_2O_2 addition. The transfer curves were obtained for various source–drain voltages (V_{ds}) from 1 to 20 V. The leakage currents in the figures were drain currents measured at $V_{ds} = 0$ V, which show that leakage currents are quite low. The extracted parameters are presented in Fig. 5 and Table I.

Figure 5(a) shows the decrease in the sub-threshold slope with increasing dilution ratio. The subthreshold slope strongly depends on the defect states near the interface and decreases with the decrease of defects. Thus, the decreased subthreshold slope means that the number of defects near the interface decreased with increasing dilution ratio. The scattering of carriers at the defect states decreases the mobility of the carriers. Therefore, it is understandable that the mobility increases owing to less scattering as the dilution ratio increases, as shown in Fig. 5(b). The defect states and viscosity are both important for carrier mobility because high viscosity easily produces voids and pinholes, which increase the scattering of carriers.

Figure 5(a) shows more improvement in the subthreshold slopes with the addition of H_2O_2. The subthreshold slope became steeper with the addition of H_2O_2, as shown in Fig. 4(b). The subthreshold slope strongly depends on the defect states at or near the interface, and a steeper slope suggests a more reduced density of defect state in the case of H_2O_2 addition.

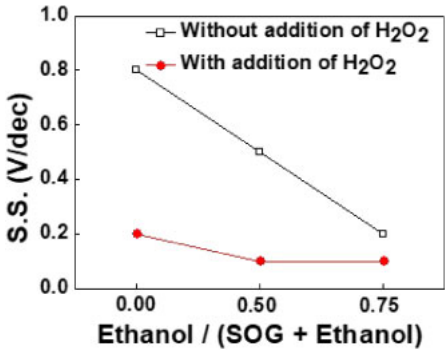

(a)

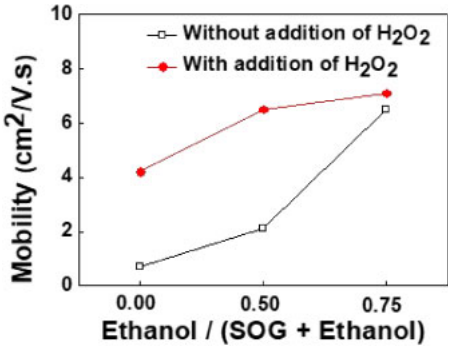

(b)

Fig. 5. (Color online) (a) Subthreshold slope and threshold voltages and (b) mobilities as a function of dilution ratio and addition of H_2O_2.

Table I. Transistor parameters according to dilution conditions.

Dilution	V_{th} (V)	S.S. (V/dec)	I_{on}/I_{off}	μ [$cm^2/(V{\cdot}s)$]
0%	5.1	0.8	5.4×10^4	0.7
50%	1.5	0.2	1.3×10^7	4.2
75%	1.1	0.5	1.1×10^5	2.1
0% with H_2O_2	1.0	0.1	2.8×10^7	6.5
50% with H_2O_2	0.8	0.2	3.3×10^7	6.5
75% with H_2O_2	0.5	0.1	3.5×10^7	7.1

SOG consists of Si–O network polymers, which are siloxane polymers dissolved in an organic solvent such as isopropyl alcohol, or ethyl alcohol. Siloxane is silicon–oxygen bonds with alkyl groups. During baking and curing after spin coating, the solvent evaporates out and siloxane polymers are cross-linked to form Si–O–Si networks. The main reaction is the cross linking of silanol to form the Si–O–Si networks. The silanol is Si–OH, which reacts with other groups to form an inorganic glass film. Therefore, as the cross-linking proceeds, the amount of silanol decreases. As the dilution ratio increases, the TFT characteristics, such as the subthreshold slope and threshold voltage and mobility were improved, which were attributed to the fewer defects or trap states in the case of using diluted SOG. As a reason of the improved characteristics, we consider that the Si–OH network enhanced by dilution in turn enhances the Si–O–Si network as a result of the condensation process, which enhance the cross-linking to reduce the number of alkyl-related defects. Addition of hydrogen peroxide improved the TFT characteristics further. Since many broken bonds are generated during the cross-linking, it is reasonable that reactive oxygen generated from a strong oxidizing agent passivates the broken bond, thereby decreasing the number of defects, which improves the subthreshold slope and mobility of carriers in the TFT.

In the case of H_2O_2 addition, the on-current deviates from linearity with increasing gate voltage, as shown in Fig. 4(b). The nonlinearity comes from the voltage drop due to the contact resistances of the source/drain regions. The voltage drop reduces the voltages to the channel region, which reduces the lateral electric field between the source and the drain. The reduced electric field decreases drain current. The starting drain currents over the threshold voltage are larger than those of TFTs without H_2O_2 addition, but the currents become smaller with increasing gate voltage.

The high on-current around low gate voltages before the influence of the contact resistance is consistent with the steep subthreshold slope in terms of the reduced number of defects near the interface. Therefore, it is considered that enough oxygen generated by the hydrolysis of hydrogen peroxide form SiO_2 effectively and reduces the number of oxygen vacancies near the interface between the oxide semiconductor and the SOG gate insulator. However, the reason for the increased contact resistance after adding hydrogen peroxide is unclear, and further research is necessary in terms of the metal oxidation at the interface by oxygen from oxidizing agent.

The surface roughness of the SOG films at various dilution ratios was measured by atomic force microscopy (AFM), and the root mean square (RMS) roughness is shown in Fig. 6. The dilution changes the viscosity of SOG, and the RMS roughness decreased from 0.73 to 0.51 nm with increasing dilution ratio, and the addition of hydrogen peroxide. The decrease in roughness results in less scattering, which in turn increases mobility.

4. Conclusions

Top-gate amorphous IGZO TFTs were developed using SOG insulators for the buffer, gate insulator, and inter-layer dielectric. The SOG solution was diluted to improve the performance. Furthermore, the addition of H_2O_2 improved the characteristics more than dilution alone. Since the solution process is free of plasma ion-induced damage, defect generation by ion bombardment can be avoided. The surface roughness of the SOG film was also improved by dilution and the addition of H_2O_2. The RMS roughness was decreased from 0.73 to 0.51 nm with increasing dilution from 0 to 75% with the addition of hydrogen peroxide, which reduces the number of pores and pinholes that act as scattering centers for carriers.

The subthreshold slope, threshold voltage, and mobility were improved with further SOG dilution and addition of H_2O_2. The improvement of the TFT characteristics by dilution was attributed to the decrease in surface roughness, compensation for oxygen vacancies, and decrease in the number of interface defects. The addition of H_2O_2 further improved the TFT characteristics owing to the strong oxidization effect. The oxygen supplied by hydrolysis of the hydrogen peroxide can enhance oxygen bonding, reduce the number of oxygen vacancies, and easily remove organic compounds. The dilution of SOG with ethanol and the

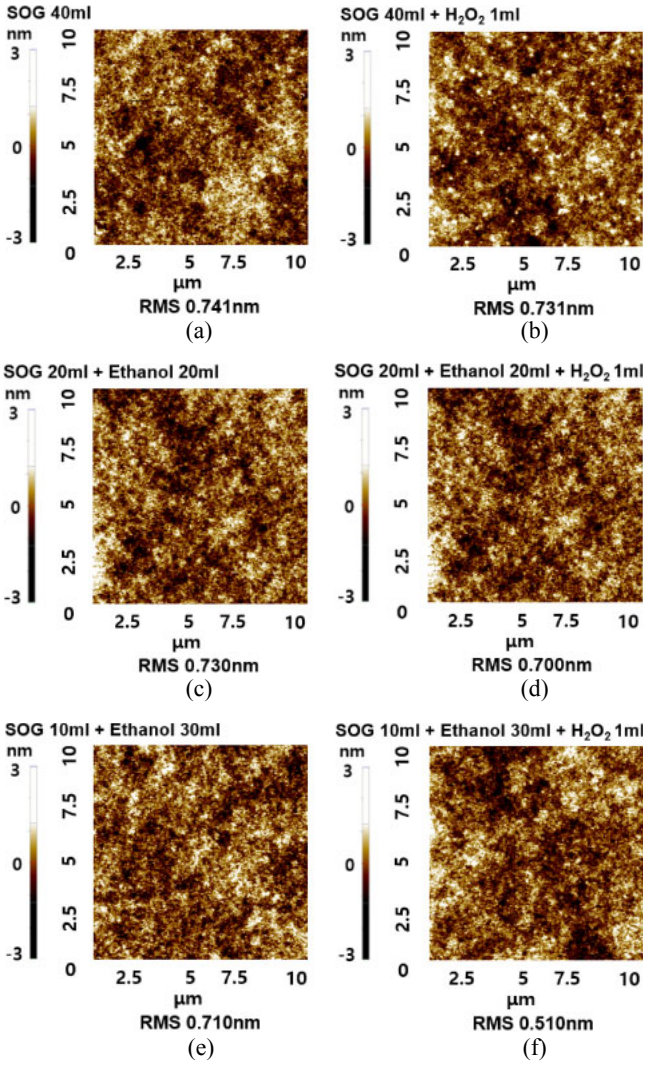

Fig. 6. (Color online) RMS roughness of each SOG film determined by AFM measurement.

addition of H_2O_2 improved the characteristics, and the subthreshold slope, threshold voltage, mobility, and on–off ratio were 0.5 V, 0.1 V/dec, 7.1 $cm^2/(V{\cdot}s)$, and 3.6×10^7, respectively.

Acknowledgment

This research was supported by Basic Science Research Program through the National Research Foundation of Korea (NRF) and funded by the Ministry of Education (2017R1D1A1A02019514).

1) C.-W. Han, J.-S. Park, H.-S. Choi, T.-S. Kim, Y.-H. Shin, H.-J. Shin, M.-J. Lim, B.-C. Kim, H.-S. Kim, B.-S. Kim, Y.-H. Tak, C.-H. Oh, S.-Y. Cha, and B.-C. Ahn, J. Soc. Inf. Disp. **22**, 552 (2014).
2) S. Yamazaki, T. Hirohashi, M. Takahashi, S. Adachi, M. Tsubuku, J. Koezuka, and S. Mori, J. Soc. Inf. Disp. **22**, 55 (2014).
3) S. Steudel, J. L. P. Steen, M. Nag, T. H. Ke, S. Smout, T. Bel, and M. Rovers, J. Soc. Inf. Disp. **25**, 222 (2017).
4) P. T. Liu, Y. T. Chou, and L. F. Teng, Appl. Phys. Lett. **95**, 233504 (2009).
5) B. Shin, J. R. Weber, R. D. Long, P. K. Hurley, C. G. Van de Walle, and P. C. Mclntyre, Appl. Phys. Lett. **96**, 152908 (2010).
6) Y. J. Tak, S. P. Park, T. S. Jung, H. Lee, W.-G. Kim, J. W. Park, and H. J. Kim, J. Inf. Disp. **17**, 73 (2016).
7) K. Nomura, A. Takagi, T. Kamiya, H. Otha, M. Hirano, and H. Hosono, Jpn. J. Appl. Phys. **45**, 4303 (2006).
8) M. Nag, K. Obata, Y. Fukui, K. Myny, S. Schols, P. Vicca, and A. Bhoolokam, SID Symp. Dig. Tech. Pap. **45**, 248 (2014).
9) H. Gleskova, S. Wagner, V. Gašparík, and P. Kováč, J. Electrochem. Soc. **148**, G370 (2001).
10) Y. Lee, J. Kim, J. N. Jang, I. H. Yang, S. Kwon, M. Hong, and W. G. Jang, Thin Solid Films **517**, 4019 (2009).
11) C. L. Fan, M. C. Shang, B. J. Li, Y. Z. Lin, S. J. Wang, W. D. Lee, and B. R. Hung, Materials **8**, 1704 (2015).
12) J. S. Seo, J. H. Jeon, Y. H. Hwang, H. Park, M. Ryu, S. H. K. Park, and B. S. Bae, Sci. Rep. **3**, 2085 (2013).
13) M. Kim, J. H. Jeong, H. J. Lee, T. K. Ahn, H. S. Shin, J.-S. Park, J. K. Jeong, Y.-G. Mo, and H. D. Kim, Appl. Phys. Lett. **90**, 212114 (2007).
14) K. Song, W. Yang, Y. Jung, S. Jeong, and J. Moon, J. Mater. Chem. **22**, 21265 (2012).
15) G. H. Gelinck, H. E. A. Huitema, E. van Veenendaal, E. Cantatore, L. Schrijnemakers, J. B. P. H. van der Putten, T. C. T. Geuns, M. Beenhakkers, J. B. Giesbers, B.-H. Huisman, E. J. Meijer, E. M. Benito, F. J. Touwslager, A. W. Marsman, B. J. E. van Rens, and D. M. de Leeuw, Nat. Mater. **3**, 106 (2004).
16) X. Liu, M. Kanehara, C. Liu, and T. Minari, J. Inf. Disp. **18**, 93 (2017).
17) T. Toda, G. Tatsuoka, Y. Magari, and M. Furuta, IEEE Electron Device Lett. **37**, 1006 (2016).
18) V. Podzorov, V. M. Pudalov, and M. E. Gershenson, Appl. Phys. Lett. **82**, 1739 (2003).
19) X. Liu, J. Emmanuel, T. Mohammed-Brahim, and W. Lei, Proc. Int. Conf. Sensing Tech., 2006, p. 12.
20) R. Usuda, K. Uchida, and S. Nozaki, Appl. Phys. Lett. **107**, 182903 (2015).
21) T. Kubo, E. Tadaoka, and H. Kozuka, J. Sol–Gel Sci. Technol. **31**, 257 (2004).
22) H. Kozuka, K. Nakajima, and H. Uchiyama, ACS Appl. Mater. Interfaces **5**, 8329 (2013).
23) D. Hishitani, M. Horita, Y. Ishikawa, H. Ikenoue, and Y. Uraoka, Jpn. J. Appl. Phys. **56**, 056503 (2017).
24) J. H. Cheon, J. H. Bae, and J. Jang, IEEE Electron Device Lett. **29**, 235 (2008).
25) J. H. Cheon, J. H. Bae, W. G. Lee, and J. Jang, Electrochem. Solid-State Lett. **11**, H77 (2008).
26) M. A. Dominguez, P. Rosales, A. Torres, and M. Moreno, MRS Proc. **1426**, 169 (2012).
27) J. J. Huang, C. J. Liu, H. C. Lin, C. J. Tsai, Y. P. Chen, G. R. Hu, and C. C. Lee, J. Phys. D **41**, 245502 (2008).
28) W. H. Jeong, D. L. Kim, and H. J. Kim, ACS Appl. Mater. Interfaces **5**, 9051 (2013).
29) A. T. Kohl, R. Mimna, R. Shick, L. Rhodes, Z. L. Wang, and P. A. Kohl, Electrochem. Solid-State Lett. **2**, 77 (1999).